Eur. Phys. J. A **22**, 163–171 (2004)
DOI 10.1140/epja/i2004-10015-y

THE EUROPEAN PHYSICAL JOURNAL A

Direct mass measurements of neutron-deficient xenon isotopes using the ISOLTRAP mass spectrometer

J. Dilling[1,2,a], F. Herfurth[3], A. Kellerbauer[3], G. Audi[4], D. Beck[1], G. Bollen[5], H.-J. Kluge[1], R.B. Moore[6], C. Scheidenberger[1], S. Schwarz[5], G. Sikler[1], and the ISOLDE Collaboration[2]

[1] GSI Darmstadt, Planckstr. 1, 64291 Darmstadt, Germany
[2] TRIUMF, 4004 Wesbrook Mall, Vancouver, B.C., V6T 2A3, Canada
[3] CERN, Division EP, 1211 Geneva 23, Switzerland
[4] CSNSM-IN2P3-CNRS, 91405 Orsay-Campus, France
[5] NSCL/MSU, East Lansing, South Shaw Lane, MI, 48824-1321, USA
[6] McGill University, Department of Physics, Montreal, H3A 2T8, Canada

Received: 15 January 2004 / Revised version: 8 April 2004 /
Published online: 3 November 2004 –
Communicated by J. Äystö

Abstract. The masses of the noble-gas Xe isotopes with $114 \leq A \leq 123$ have been directly measured for the first time. The experiments were carried out with the ISOLTRAP triple trap spectrometer at the on-line mass separator ISOLDE/CERN. A mass resolving power of the Penning trap spectrometer of $m/\Delta m$ of close to a million was chosen resulting in an accuracy of $\delta m \leq 13$ keV for all investigated isotopes. Conflicts with existing, indirectly obtained, mass data by several standard deviations were found and are discussed. An atomic mass evaluation has been performed and the results are compared to information from laser spectroscopy experiments and to recent calculations employing an interacting boson model.

PACS. 07.75.+h Mass spectrometers – 21.10.Dr Binding energies and masses – 27.60.+j $90 \leq A \leq 149$ – 32.10.Bi Atomic masses, mass spectra, abundances, and isotopes

1 Introduction

Ground-state nuclear properties of atoms, such as binding energies or particle separation energies are accessible via mass measurements. The information gained allows to test models of the nucleus and underlying nuclear structure. Deviations of the model would directly be apparent in comparison with the experimental results. Recent progress in the theoretical sector, for example in shell-model calculations, demands more and often specific mass information, to check and further develop the used model. This is most crucial for theoretical descriptions that are based on a global and a local part, such as the interacting boson model (IBM) [1]. Moreover, progress in the last 5–10 years in the experimental sector, firstly in the production and availability of exotic nuclides, and secondly in mass measurement techniques, particularly for short-lived species, allows one to provide a large variety of high-quality mass measurement data. In one sequence of previous measurements we have concentrated on neutron-deficient isotopes of Hg, Pb, Bi, and Po [2]. The focus was due to interesting nuclear structure in this region in the vicinity of doubly magic numbers. In the here presented measurements on neutron-deficient xenon isotopes, the interest lays in checking the theoretical modelling of mid-shell crossing.

2 Experimental setup and measurement procedure

The ISOLTRAP Penning trap spectrometer [3–5] is installed at the on-line facility ISOLDE/CERN [6] in Geneva, where exotic nuclei are produced via pulsed proton bombardment of a target. The produced nuclei evaporate out of the target and are subsequently ionized, extracted and mass separated. The quasi-continuous beam with typically 30–60 keV is delivered to the experiments, one of which is the ISOLTRAP spectrometer.

The ISOLTRAP experiment consists of three electromagnetic traps which all serve specific purposes. The first trap is a linear radiofrequency quadrupole (RFQ) trap [5] which is used to stop, cool and transform the continuous beam into a low-energy ion bunch. The second trap is a cylindrical Penning trap, which acts as an isobar separator [7]. The third trap is a hyperbolic Penning trap

[a] e-mail: JDilling@triumf.ca

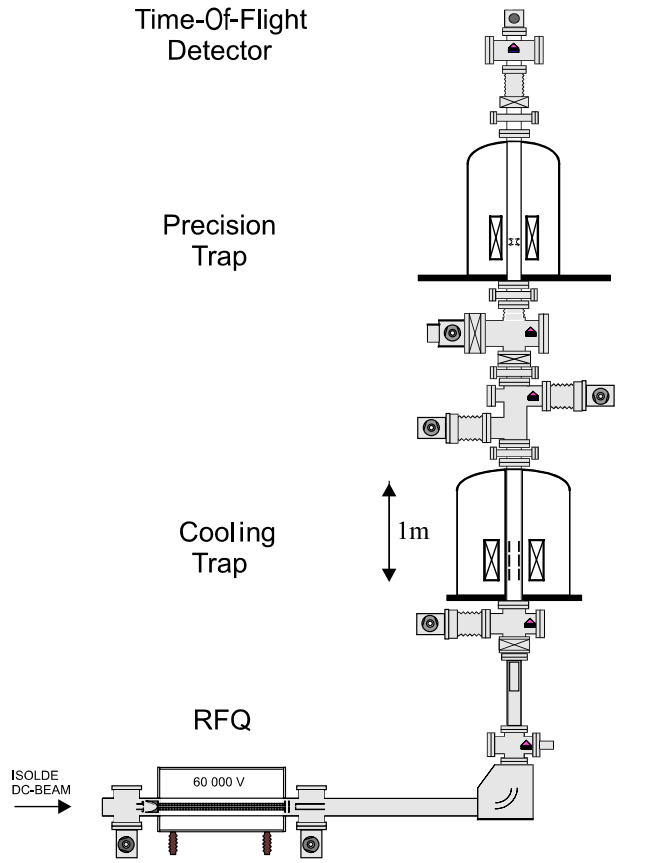

Fig. 1. Experimental setup of ISOLTRAP. The linear Paul (RFQ) trap is used for cooling and bunching of the ISOLDE beam. The cooling trap acts as an isobar separator. The mass measurement is performed with the precision trap and employing a time-of-flight technique.

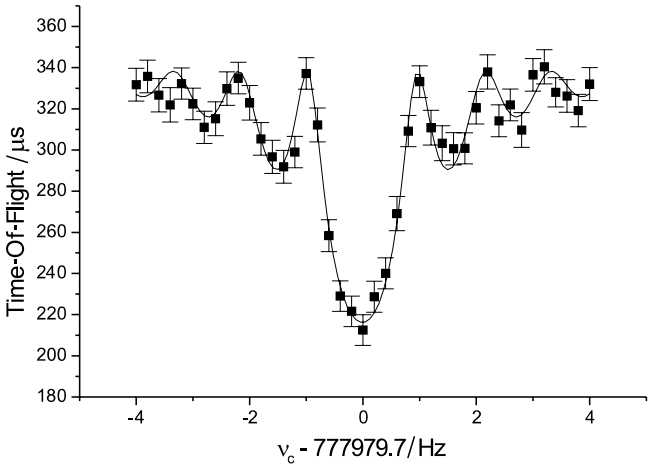

Fig. 2. Cyclotron resonance curve for ^{117}Xe. Depicted is the time of flight of the ions from the trap to a detector as a function of applied radiofrequency. The solid line is a fit of the theoretically expected shape [10] to the experimental points.

employed as the high-accuracy mass spectrometer. Figure 1 shows the setup of the triple-trap spectrometer.

The RFQ trap is operated on a 60-kV high-voltage platform and accepts the electrostatically retarded ISOLDE beam. Interactions of the ions with the buffer gas cool them to the ambient temperature. Switchable potentials allow for a three-dimensional trapping, hence for an accumulation of the cooled ions, which can then be extracted as a bunched beam. A drift-tube with fast-adjustable potentials allows for a tailoring of the kinetic transfer energy of the ion bunch [5].

The second trap is a cylindrical Penning trap and is used to further clean the ion sample, by applying a mass-selective buffer gas cooling technique [3,7]. From here the ions are gently extracted and delivered to the third trap.

The third trap is a precision Penning trap with hyperbolic electrode configuration, in which the precision mass measurement is performed [4]. This is done by measuring the time of flight (TOF) of the released ions from the trap to a detector. The flight time is depending on the initial energy of the ions in the trap, which is composed of a longitudinal and radial part. The latter one can be maximized by applying an azimuthal quadrupole RF-field in the trap at the resonance frequency ν_c. The ions are then released from the trap and drift towards a particle detector. During this drift through the inhomogeneous part of the magnetic field the radial energy is converted to axial energy. Therefore the ions with the largest radial energy, hence the ions previously prepared at resonance with ν_c, reach the detector faster. In this way, the TOF from the trap to the detector can be used to determine the cyclotron frequency [8].

The equation

$$\nu_c = q/m \cdot B/2\pi, \tag{1}$$

relates the cyclotron frequency ν_c to the charge-to-mass ratio q/m of the ions under investigation. The magnetic field B is calibrated by use of a reference nuclide whose mass is well known. Ideally, ions of isotopically pure carbon ion-cluster C_x are employed [9], eliminating an error for this mass, since carbon-12 is used for the definition of the unified atomic mass unit u.

Only singly charged ions are delivered to the precision trap, therefore the knowledge of the magnetic field strength allows one to unambiguously determine the mass of the ions. Figure 2 shows an example of a time-of-flight spectrum as a function of applied radiofrequency. The solid line is the theoretically expected shape of the resonance [10] fitted to the data points. The resonance width $\Delta\nu_{\mathrm{FWHM}}$ is approximately equal to the inverse of the excitation period T_{RF} [11]. For example for $A = 120$ the cyclotron frequency is $\nu_c = 760$ kHz in a magnetic field of $B = 6$ T. Exciting the ions for a duration of $T_{\mathrm{RF}} = 900$ ms leads to a width of $\Delta\nu_{\mathrm{FWHM}} \approx 1.1$ Hz. This corresponds to a resolving power $R = 690000$, allowing mass measurements with a relative uncertainty of $\delta m/m \approx 1 \cdot 10^{-7}$, which was the aim of these experiments.

Table 1. List of the investigated xenon isotopes. Tabulated are the frequency ratios including statistical and total uncertainty, with respect to the reference measurements of ^{133}Cs. The half-life and the maximum number of detected ions per cycle are given. The next two columns show the mass excess from the Penning Trap (ME PT) frequency ratio and the literature value (ME AME) from the 1995 Atomic Mass Evaluation [17] together with the corresponding absolute uncertainty. Values marked (#) are estimates from systematic trends [17]. In the last column the deviation between those two values is shown.

Nuclide	Freq. Ratio ν_{ref}/ν	$T_{1/2}$	No. ions	ME PT (keV)	ME AME 95 (keV)	Dev (keV)
^{114}Xe	0.8572101482 (34) (93)	10 s	1	−67086 (12)	−66933 # (207#)	−153
^{115}Xe	0.8647216374 (32) (95)	18 s	1	−68657 (12)	−68426 # (239#)	−231
^{116}Xe	0.8722103533 (42) (109)	59 s	1	−73047 (13)	−72901 # (246#)	−146
^{117}Xe	0.8797253356 (19) (91)	61 s	9	−74185 (11)	−73994 (180)	−191
^{118}Xe	0.8872180141 (24) (93)	3.8 m	8	−78084 (12)	−77710 (1000)	−374
^{119}Xe	0.8947364709 (33) (91)	5.8 m	5	−78792 (11)	−78660 (123)	−133
^{120}Xe	0.9022333721 (40) (102)	40 m	1	−82169 (13)	−81832 (44)	−338
^{121}Xe	0.9097551270 (33) (100)	40.1 m	4	−82469 (12)	−82539 (24)	70
^{122}Xe	0.9172560020 (29) (99)	20.1 h	10	−85354 (12)	−85185 (87)	−169
^{123}Xe	0.9247811247 (40) (100)	2.08 h	4	−85237 (12)	−85260 (15)	23
^{124}Xe	0.9322857418 (22) (97)	stable	9	−87658 (12)	−87658 (2)	0
^{130}Xe	0.9774128763 (27) (101)	stable	8	−89878 (13)	−89881 (1)	3

3 Measurements

The data in this work have been obtained during one on-line run over a period of 28 hours. A La_2O_3 target was bombarded by a 1-GeV proton beam with an averaged current of 1 μA. The target was coupled via a cold transfer line to a plasma ion source. In this way contamination of the beam with non-volatile elements was drastically reduced. The ISOLDE facility offers two magnetic separators. Here, the general purpose separator (GPS) [12] was used, with a mass resolving power of about $R = m/\Delta m_{\mathrm{FWHM}} \approx 800$. Since this resolving power does not assure the removal of all isobaric contaminations, the ion sample has to be further processed in the cooling Penning trap. Isobars of Cs, In, Sn, I and even molecules like InO have to be considered as contaminants in the ion sample. However, the well-established [7] cleaning procedure in the cooling Penning trap with a resolving power of $R \approx 70000$ allows one to deliver a clean sample to the precision Penning trap.

Mass measurements of neutron-deficient xenon isotopes with $114 \leq A \leq 123$ and of stable xenon isotopes with $A = 124, 130$ were carried out in the present experiment. The measurement procedure includes the preparation in the RFQ trap (10 ms), the purification in the cooling trap (120 ms) and the measurement in the precision trap (900 ms). In the last step the ions are excited by an RF-field at a given frequency and then released towards the detector for the time-of-flight measurement. The complete cycle is then performed 41 times for equidistant RF-frequencies in order to determine the resonance frequency.

3.1 Frequency ratios

The cyclotron frequency is obtained by fitting the theoretical shape of the resonance [10] to the measured data points (fig. 2). The center frequency, the FWHM, and the statistical uncertainty is deduced. For the conversion into an atomic mass the magnetic field has to be known. This is accomplished by measuring the cyclotron frequency ν_{ref} of stable ions with very well-known mass. In this case ^{133}Cs was used, particularly for the following three reasons: the mass was recently determined [13] with a relative uncertainty of $\delta m/m = 2 \cdot 10^{-10}$, secondly the mass difference between the reference ions and the xenon ions is small, allowing one to map out essentially the same ion trajectory space in the trap, and as a last point due to the availability in form of isobaric clean beams from our internal test ion source independently of the ISOLDE facility.

The ratio of the two measured frequencies $r = \nu_{\mathrm{ref}}/\nu$ is given as the primary experimental result. Table 1 shows the measured isotopes together with the frequency ratio with respect to ^{133}Cs ions. Shown in the first parenthesis is the statistical and in the second the total uncertainty. The statistical uncertainty depends on the number of detected ions, which was on average $\bar{N} \approx 5000$ per isotope. Including the resolving power of the spectrometer, the expected statistical uncertainty can be approximated as [11]

$$\delta\nu/\nu = 1/R \cdot 1/\sqrt{\bar{N}} = 2 \cdot 10^{-8}. \quad (2)$$

The total uncertainty is given as the quadratic sum of the statistical uncertainty and the systematic error. Sources of systematic errors to be considered are the following:

- Frequency shift due to field imperfections. These systematic errors are proportional to the mass difference between the reference ions and the ions under investigation. This difference is at maximum δA =19 amu (for ^{114}Xe). For ISOLTRAP this shift is $1.6{\cdot}10^{-10}$/amu [14] corresponding to a maximum shift of $3 \cdot 10^{-9}$.
- Contaminants in the measurement trap. Investigations at ISOLTRAP [15] showed that these effects start to influence the results on a level aimed for here, with 15

Table 2. Results of the new atomic mass evaluation. The mass excess (ME) values from two least-squares adjustment are given (AME 95 and AME_{new} including the Penning trap data) with the total unceratinty in parenthesis. The deviation between both is listed in the last column. Values marked with # are estimations from systematic trends [17]. Besides the measured isotopes, those changed in mass value in the new AME by more than 5 keV are tabulated.

Nuclide	ME AME 95 (keV)	ME AME new (keV)	Dev (keV)
^{114} Xe	−66933.0 # (207.0#)	−67086.2 (12.0)	−153
^{115} Xe	−68426.0 # (239.0#)	−68656.0 (12.0)	−231
^{116} Te	−85305.7 (92.0)	−85288.3 (95.0)	14
^{116} I	−77560.5 (142.6)	−77543.2 (144.6)	17
^{116} Xe	−72901.0 # (246.0#)	−73047.0 (13.0)	−146
^{117} I	−80436.5 (71.1)	−80447.1 (72.4)	−11
^{117} Xe	−73993.6 (179.9)	−74184.7 (11.0)	−191
^{117} Ba	−56952.0 # (648.0#)	−57098.0 # (600.0#)	−146
^{118} Xe	−77709.7 (1000.1)	−78084.7 (11.0)	−375
^{119} I	−83666.0 (63.4)	−83671.5 (64.8)	−6
^{119} Xe	−78659.9 (123.4)	−78792.0 (11.0)	−133
^{119} Ba	−64220.8 (1019.9)	−64595.8 (200.3)	−375
^{120} Xe	−81831.5 (44.0)	−82169.5 (13.0)	−338
^{121} Xe	−82539.3 (24.4)	−82468.9 (12.0)	70
^{121} Cs	−77139.3 (13.9)	−77068.9 (23.4)	70
^{121} Ba	−70342.5 (303.2)	−70680.6 (300.3)	−338
^{122} Xe	−85185.2 (87.3)	−85354.5 (12.0)	−169
^{123} Xe	−85259.9 (15.4)	−85245.5 (9.0)	14

ions detected simultaneously at the particle detector. This was prevented by having always very few ions in the precision trap. Table 1 shows the maximum allowed number of detected ions per cycle.

– Variations of the magnetic field, for example due to changes of air pressure or ambient temperature. Typically a day-night shift of $\delta B/B \approx 1 \cdot 10^{-7}$ was found [16]. The measured average variation in the present experiments was $\delta B/B = 3 \cdot 10^{-8}$ for 11 reference measurements during the 28 hours duration of the experiment.

The total contribution of these systematic errors is below $1 \cdot 10^{-7}$. Nevertheless, this is taken as a conservative estimate for systematic errors, and is added quadratically to the statistical uncertainty.

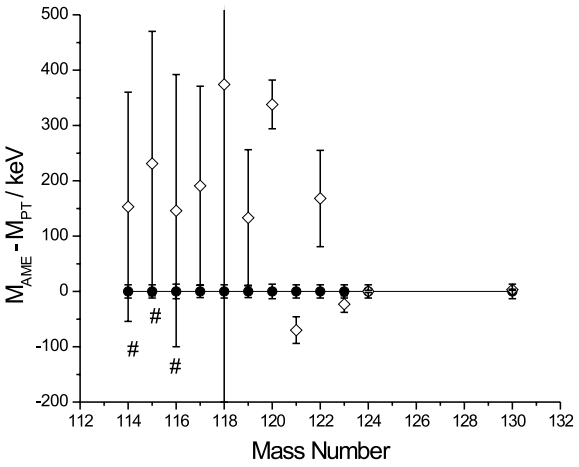

Fig. 3. Difference between xenon mass values from the Atomic Mass Evaluation 1995 (AME) [17] (open symbols) and an evaluation including the ISOLTRAP data (filled circles on zero-line). For isotopes marked with # masses are estimated from systematic trends [17].

3.2 Mass values

The conversion of the frequency ratio into an atomic mass m is done by multiplying the ratio with the mass of the reference ion m_{ref}, and adding the rest mass of the electron m_e,

$$m = (\nu_{ref}/\nu) \cdot m_{ref} + m_e. \quad (3)$$

Using the frequency ratio and the known mass of the reference ions, the mass can be given as a secondary experimental result. The mass excess (ME) derived from that relation is given in table 1 together with the final uncertainty. Also, the mass excess from literature values [17] or estimates from systematic trends, are listed.

The masses of the three isotopes ^{114}Xe, ^{115}Xe and ^{116}Xe were determined for the first time. For all measured unstable xenon isotopes the accuracy was drastically improved. The reliability and accuracy of the ISOLTRAP measurement could be demonstrated in the cases of the stable isotopes ^{124}Xe and ^{130}Xe, which are known with an accuracy of about $1 \cdot 10^{-8}$. The deviation

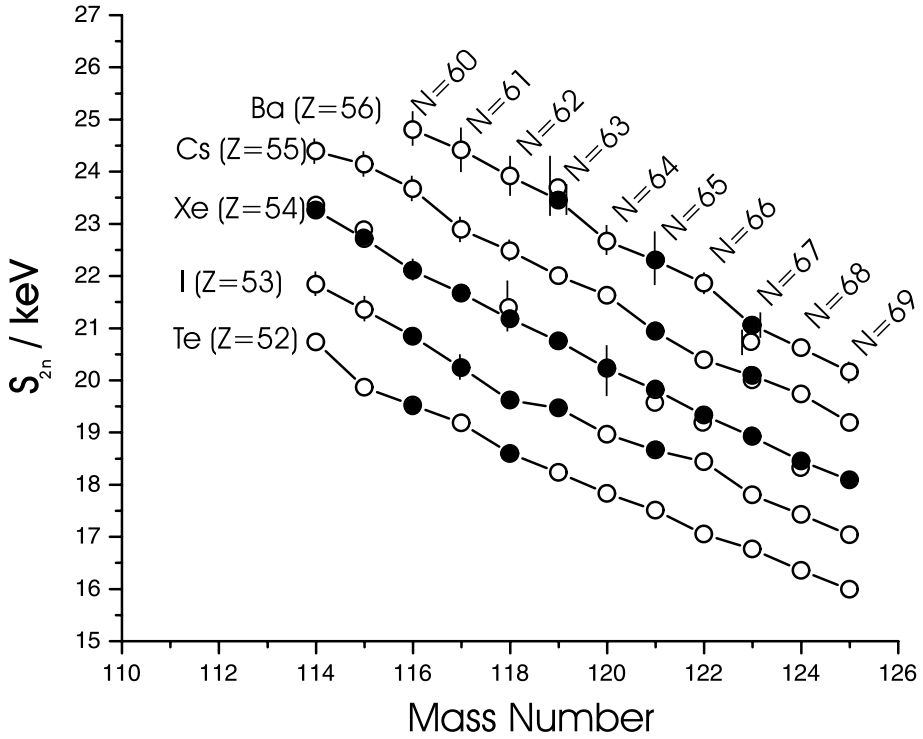

Fig. 4. Two-neutron separation energy as a function of mass number A. Filled circles show the new values, open circles previous data calculated from AME 95 [17]. For values with uncertainties smaller than 300 keV, the error bar is hidden. The error bars at filled circles in general belong to the previous value underneath. For two barium isotopes, the uncertainty has changed and is still displayable; here the error bar on the left of the circle indicates that of AME 95 and the one on the right side that of the AME performed in this work.

of the ISOLTRAP data from those values is $\delta m(^{124}\mathrm{Xe}) = 0(12)$ keV and $\delta m(^{130}\mathrm{Xe}) = 3(13)$ keV, hence excellent agreement is observed.

4 Atomic mass evaluation and results

Within this work an atomic mass evaluation (AME) has been performed. A detailed description of such an evaluation can for example be found in the tables of 1995 [17] (in the following called AME 95) or in the most recent version of 2003 [18]. The experimental data derived here were included in the evaluation AME 2003, and results presented here are identical to the data given therein. The concept of such an evaluation is to use all available experimental mass data for a least-squares procedure of linear equations. Table 2 gives the result of the atomic mass evaluation. Listed are all nuclides whose mass value changed compared to AME 95 by more than 5 keV when including the new ISOLTRAP data. From the 12 directly measured xenon isotopes a total number of 18 nuclides where found to be influenced notedly. For the xenon isotopes themselves, some drastic shifts occurred in the mass values, going up to 7.7 standard deviations compared to the previous values of the AME 95. Figure 3 shows the difference of the atomic evaluation with and without the ISOLTRAP data. One clearly notices a dramatic improvement in accuracy with the new ISOLTRAP values. For all measured xenon isotopes a mass uncertainty on the order of $\delta m \leq 13$ keV could be reached. For the xenon isotopes with $A = 114, 115$ and 116 only estimated values existed, which could now be replaced by precise experimental data. It is, however, notable that those values estimated in AME 95 agree well within their (large) error bars with the now measured values. This is in contrast to previously experimentally determined xenon masses closer to the valley of stability. Also, one notices that most of the previous mass values were too large, which is in most cases due to erroneous mass assignments from underestimation of contributions of contaminants. A detailed comparison between old and new input data is discussed in the Appendix, solving also the conflicts of the deviations found.

5 Discussion of the results of the new atomic mass evaluation

5.1 Two-neutron separation energies (S_{2n})

The S_{2n} is defined as the difference in binding energy of a nucleus ($E^B(Z,N)$) *versus* the binding energy of a nucleus with two neutron less by

$$S_{2n} = E^B(Z,N) - E^B(Z,N-2). \quad (4)$$

The visualization of the two-neutron separation energy allows one to recognize changes in the nuclear structure

without the complication of effects such as pairing. The advantage is to see the influence of single changed values in the context of an isotopic chain, and to spot irregularities from clear trends. Figure 4 shows the S_{2n} as a function of mass number A for the measured xenon chain and element chains, where changes occurred due to ISOLTRAP data. This is the case for 23 S_{2n}-values, where at least one datum of the S_{2n} input was changed. The new values are plotted as filled circles, the previous data taken from the AME 95 as open circles. Generally, a very smooth behaviour of the two-neutron separation energies (especially for the nuclides with even proton number) is found in this region of the chart of nuclides. This indicates the absence of any drastic nuclear structure effects in those neutron mid-shell nuclides. However, at the neighboring chains of xenon some local irregularities appear, like in the case of ^{116}Cs at $N = 61$. For this isotope the binding energy is experimentally known with an uncertainty of $\delta m = 351$ keV. The corresponding value of ^{114}Cs is a systematic estimate with $\delta m = 305$ keV. That might also be the reason for the deviation at ^{118}Cs at $N = 63$, for which the ^{116}Cs datum is also used.

Another case for such a deviation from the general trend is found at ^{118}I with $N = 65$. Here the experimental uncertainty of the two isotopes which are used to derive the S_{2n} is $\delta m = 144$ keV and $\delta m = 72$ keV, respectively. For those cases experimental data with better precision would be desired.

5.2 Deformation effects within the xenon chain

Figure 5 (bottom) shows the two-neutron separation energies for xenon isotopes with $114 \leq A \leq 141$. Besides the strong discontinuity observed at the shell closure at $N = 82$, a smoothly varying two-neutron separation energy is observed in the region $58 \leq A \leq 82$.

Information on the quadrupole deformation can be obtained from isotope shift measurements via collinear laser spectroscopy [19]. Figure 5 (top) shows the mean charge radius difference $\delta\langle r^2\rangle$ as a function of neutron number N or mass number A. Shown are also equideformation lines of $\langle\beta_2^2\rangle^{1/2}$-values at 0.1, 0.2 and 0.3 as calculated by use of the droplet model [20]. Comparing the S_{2n} values with $\delta\langle r^2\rangle$, both graphs show a similar smooth trend from the very neutron-deficient isotopes towards the shell closure at $N = 82$ where a drastic change appears. Visible is in both cases a weak odd-even staggering. The gradually increasing deformation for neutron number below $N = 82$ as obtained from the isotope shift data is reflected in the light curvature of the S_{2n} values. No signature for a sudden transition appears neither in the isotope shift nor in the mass data. This is consistent with the description of a "soft"-core by T.R. Werner and J. Dudek [21]. Shape coexistence by a particle-hole intruder configuration is one of the suggested models for the enhanced $E0$ and $E2$ transition rates in the midshell Xe isotopes, particularly at $N = 64, 66$ and 68, found by P.F. Mantica and W.B. Walters [22]. Indications for such behaviour would be deviations from a smooth trend in the S_{2n} values, which are not observed, or the often found isomerism (see [2] and references therein). No indications for isomeric states were observed by the ISOLTRAP measurements which would have been able to resolve states with excitation energies higher than 150 keV employing an RF interaction time of $T_{\mathrm{RF}} = 900$ ms. However, the possibility of shape coexistence cannot be ruled out. Further experiments are needed.

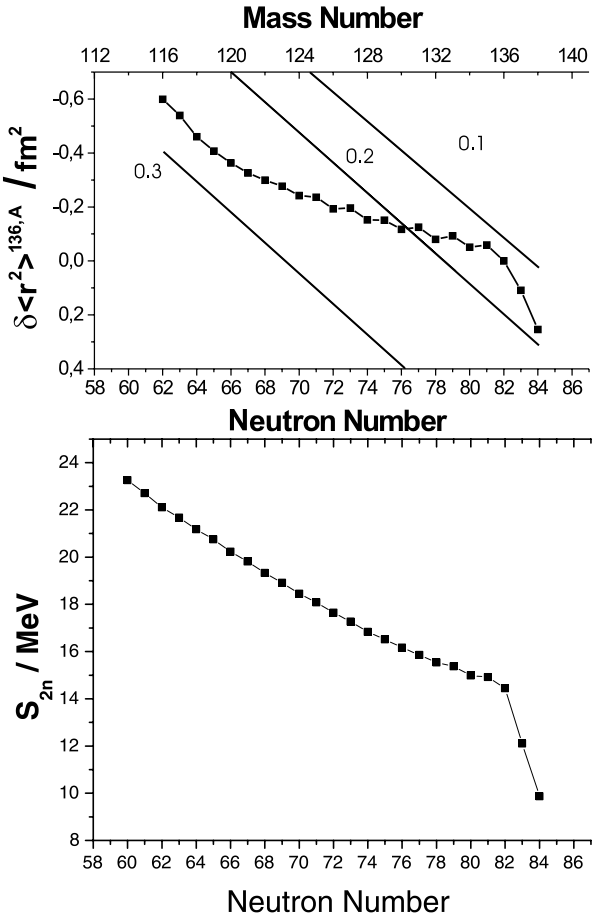

Fig. 5. Top: changes of mean square charge radii of xenon isotopes with respect to ^{136}Xe (taken from [19]). Shown are also equideformation lines for the quadrupole deformation parameter $\langle\beta_2^2\rangle^{1/2}$-values at 0.1, 0.2 and 0.3 as calculated from the droplet model [20]. Bottom: two-neutron separation energies for xenon isotopes derived from the measured mass data and AME 95.

5.3 Comparison of the experimental S_{2n} values with model predictions

The experimental results can be compared to theoretical descriptions of the interacting boson model (IBM). The model employs a global and a local formalism, where the global part describes the overall binding-energy behavior and the local part makes adjustments, particulary to asymmetric and shell-structure–based behavior. A recent investigation [23] focused on nuclei located in the 50–82 shell, hence including the relevant xenon isotopes. The

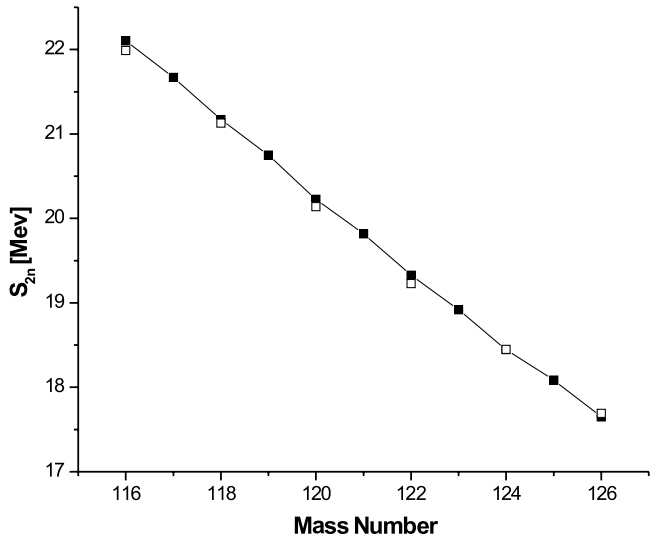

Fig. 6. Comparison between two-neutron separation energies for xenon isotopes derived from the new AME data (full squares) and theoretical predictions (open squares) calculated by use of the interacting boson model [23].

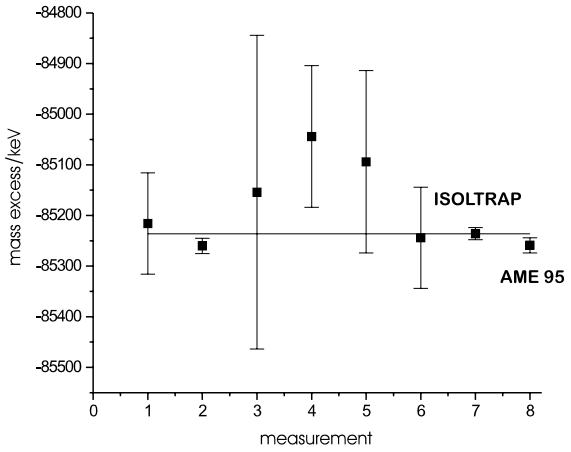

Fig. 7. Comparison of the ISOLTRAP value for ^{123}Xe with previous data of the mass excess and AME 95. The line indicates the value reported in this work. Measurement No. 1 [25], No. 2 [26], No. 3 [27], No. 4 [28], No. 5 [29], No. 6 [30].

IBM allows only the calculation of Xe nuclei with even neutron number, since it is based on bosonic configurations. Figure 6 shows the two-neutron separation energy as calculated with the binding energies from the new AME, and theoretical predictions taken from [23]. The experimental uncertainty for the S_{2n}-values is small compared to the scale and subsequently not displayed as error bar. The overall discrepancy between the experimental and model values for the shown data is $\delta E_{\mathrm{RMS}} = 155$ keV, hence is in good agreement.

6 Conclusion and outlook

The unstable xenon isotopes with $114 \leq A \leq 123$ have been directly measured using the ISOLTRAP triple trap spectrometer. The experimental precision that could be reached is increased drastically compared to the previous data, and is now $\delta m \leq 13$ keV for all nuclei investigated. For the isotopes ^{114,115,116}Xe values estimated from systematic trends, had to be used before in the tables of the AME. These are now replaced by experimental data. An atomic mass evaluation was performed and discrepancies to the existing data were found, going up to several standard deviations. These conflicts are discussed in detail in the Appendix and are solved. The new direct and indirect mass results are used to describe the mass landscape in the S_{2n}-picture. The measured xenon isotopes follow smoothly the general trend. Other chains show local deviations which might be due to large experimental uncertainties. This lack of precision could basically be overcome with the present ISOLTRAP setup [14,24]. Isotopes like ^{116}Cs or ^{114}Cs with half lives $T_{1/2} = 700$ ms and $T_{1/2} = 570$ ms are within reach of the experiment. A comparison of the reduced S_{2n} values with even changes of mean square charge radii shows the same trends in nuclear structure. The results of recent model calculations employing the interacting boson model and the experimental results show good agreement.

The authors like to thank J.E.G. Ramos for providing the separation energies as calculated with IBM and useful discussion. Furthermore, we would like to acknowledge the support by the European Commission (EUROTRAPS FMRX-CT-97-0144 and the RTD projects EXOTRAPS FMGC-ET-98-0099 and NIPNET HPRI-CT-2001-50034).

Appendix A.

Discussion of the new input data set

In this section a detailed comparison between existing measurements and the new ISOLTRAP data is performed. All publications used or documented in previous atomic mass evaluations [17] were taken into account. For the evaluation the available data are therein carefully checked and categorized with regard of quality or documentation. In the evaluation the values are weighted in the linear equations accordingly.

^{123}Xe: For ^{123}Xe six previous mass measurements were used for the adjustment of the AME 95 [17]. All were β-endpoint determinations. No significant discrepancy is found. The most accurate one by R.B. Moore [26] (see fig. 7 value No. 2) had the most influence in the AME 95 and deviates only by $1.5\,\sigma$ from the ISOLTRAP datum (see fig. 7 value No. 7). For a second measurement there is also a $1.4\,\sigma$ deviation (see fig. 7 value No. 4). This datum is derived by K. Sofia *et al.* [28] by a linear fit to a Fermi-Kurie plot. The beta-spectrum is taken in coincidence with the 596.5 keV γ-line. The assigned uncertainty

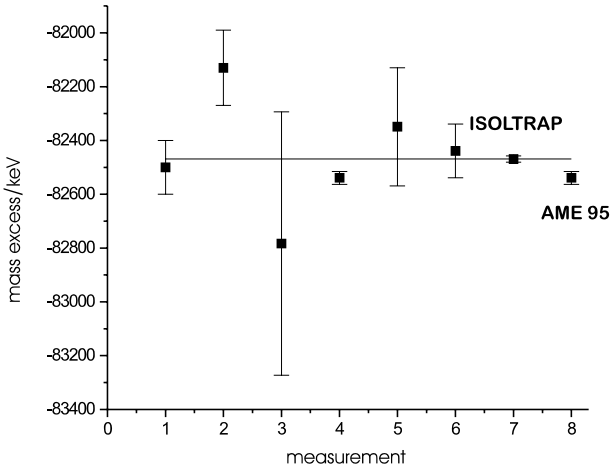

Fig. 8. Comparison of the ISOLTRAP value for ^{121}Xe with previous data of the mass excess. The line indicates the ISOLTRAP value. Measurement No. 1 [26], No. 2 [31], No. 3 [27], No. 4 [28], No. 5 [29], No. 6 [30].

seems too small, since it looks possible on the viewgraph to fit linear functions to the data points, leading to endpoints outside the error interval. The other values for this isotope agree well with the ISOLTRAP datum within their error bars. For the new atomic mass evaluation the values given in [26] and [28] are excluded from the adjustment and marked with "Well-documented data which disagree with other well-documented values".

^{122}Xe: Five endpoint measurements were performed prior to the ISOLTRAP mass measurement of which two concern the very same experiment but different corrections concerning the isomeric state of the mother nucleus. One of those corrections [29] disagrees with our datum. The documentation of this experiment, a PhD Thesis of the University of California, Berkeley, by R. F. Parry was not available, therefore a judgment of the quality was not possible. A discrepancy is found also with the experiment reported by G.D. Alkhazov *et al.* [30]. Here the technique of β-decay energies determination via γ-ray endpoints was used, where a cascade of γ-rays is summed up in an total absorption detector. For this determination it is necessary to fully understand the beta-decay strength function $S_\beta(E)$ which is not the case for this isotope. Therefore, this value is disregarded for the evaluation. The other experiments agree well within the given uncertainty.

^{121}Xe: Four of the six previously performed mass measurements of this nucleus agree well with the ISOLTRAP value. All of them are β-endpoint data. Disagreement is found with a measurement of E. Beck *et al.* [31] (see fig. 8 value No. 2). Very little information can be found in the original publication. The method used is the least-squares fit to the Fermi-Kurie plot, but it is not reported whether coincidences were used or in what way the calibration of the detector system was done. Another deviation from the ISOLTRAP datum is found in a measurement of K. Sofia *et al.* [28] (see fig. 8 value No. 4). Looking more closely at the original publication, it is obvious that the assigned uncertainty is too small. The Fermi-Kurie plot was fitted using two different binnings and the final Q_β value is the weighted mean of the two. Also the statistic particularly near the endpoint is very poor. No information is given whether the background is subtracted, which might shift the endpoint. In the same publication the identical method applied (here even with γ-coincidence) to other nuclei leads to an uncertainty seven times higher ($\delta E(^{121}\mathrm{Xe}) = 20$ keV, for $\delta E(^{123}\mathrm{Xe}) = 140$ keV). The value taken for AME 95 is the weighted mean of those measurements. They are now excluded from the evaluation and marked as "Well-documented data which disagree with other well-documented values".

^{120}Xe: For ^{120}Xe five mass measurements were carried out before. One of them was exclusively (see fig. 9 value No. 1) used for the AME 95. However, the uncertainty value was modified from the original publication of F. Münnich *et al.* [32] where the assigned uncertainty is 200 keV and the one used for AME 95 is 40 keV. The Q_β-determination method applied here is a measurement of the EC/β^+-ratio. This is based on various assumptions like that energy and parity of the ground state of ^{120}I are well known and also that there is no feeding by other more abundant β^+-decays of this state which would consequently change that rate. Further discussion with the authors of AME 95 [33] led to an exclusion of this value, due to some uncertainties of those assumptions. The other masses agree well within error bars (see fig. 9 value No. 3 and No. 5) or the uncertainty in the original publication seems to be too small. The latter is the case for [34] (see fig. 9 value No. 2) where the value is derived by a linear fit to a Fermi-Kurie plot. For the other disagreeing value (No. 4) no documentation is available [29].

^{119}Xe: The mass of this isotope given in the atomic mass evaluation of 1995 is the weighted average of two measurements [31] and [29]. Both values and the average agree well within errors with the datum presented here.

^{118}Xe: The value of ISOLTRAP is in agreement with the measured value [35] taken for AME 95. Another measurement [31] with smaller uncertainty is excluded and marked: "Data from incomplete reports, at variance with other data or with systematics" in the documentation of the new AME, due to little information given in the publication.

^{117}Xe: Two measurements were performed on the mass of this isotope. The ISOLTRAP datum agrees well with the previous data [36] and [37].

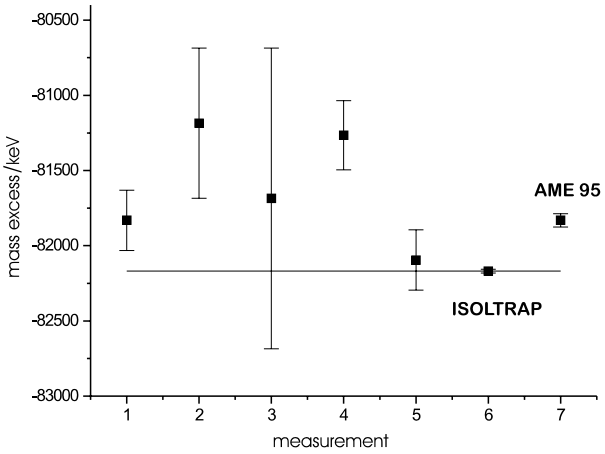

Fig. 9. Comparison of the ISOLTRAP value for ^{120}Xe with previous data of the mass excess. The line indicates the center value of the value reported in this work. Measurement No. 1 [32], No. 2 [34], No. 3 [38], No. 4 [29], No. 5 [30].

^{116}Xe: In the AME 95 an estimate from systematic trends is given. There existed, however, a measurement by Gowdy *et al.* [39] where the value is derived from the difference of two Fermi-Kurie plots. For the AME 95 this value was regarded as differing to much from the systematic trend and therefore marked as "Nuclei for which masses estimated from systematic trends are thought better than the experimental masses". Our experimental datum agrees with the value from systematics within the estimated uncertainty of the extrapolation.

^{115}Xe: For the isotope ^{115}Xe there were two values documented [38,40] in the AME 95, but the given mass is an estimation from systematic trends. The experimental masses were regarded as not reliable enough. The ISOLTRAP value agrees well with these measurements and the value derived from systematic trends. By looking at the original publication of D'Auria *et al.* [38] it seemed that the datum used in the tables is the one from systematic prediction in their work, and not their measured value. For the new documentation this is changed to a mass 400 keV more bound as this is read out from the graph.

^{114}Xe: No measurements existed for this isotope. The mass reported in this work is within the expectation from systematics.

References

1. F. Iachello, A. Arima, *The Interacting Boson Model* (Cambridge University Press, Cambridge, 1987).
2. S. Schwarz *et al.*, Nucl. Phys. A **693**, 533 (2001).
3. H. Raimbault-Hartmann *et al.*, Nucl. Instrum. Methods B **126**, 378 (1997).
4. G. Bollen *et al.*, Nucl. Instrum. Methods A **368**, 675 (1996).
5. F. Herfurth *et al.*, Nucl. Instrum. Methods A **469**, 254 (2001).
6. E. Kugler, Hyperfine Interact. **129**, 23 (2000).
7. G. Savard *et al.*, Phys. Lett. A **158**, 247 (1991).
8. G. Gräff, H. Kalinowski, J. Traut, Z. Phys. A **297**, 35 (1980).
9. K. Blaum *et al.*, Eur. Phys. J. A **15**, 245 (2002).
10. M. König *et al.*, Int. J. Mass. Spectrom. Ion. Processes **142**, 95 (1995).
11. G. Bollen, Nucl. Phys. A **693**, 3 (2001).
12. E. Kugler *et al.*, Nucl. Instrum. Methods B **70**, 41 (1992).
13. M.P. Bradley *et al.*, Phys. Rev. Lett. **83**, 4510 (1999).
14. A. Kellerbauer *et al.*, Eur. Phys. J. D **22**, 53 (2003).
15. G. Bollen *et al.*, Phys. Rev. C **46**, R2140 (1992).
16. D. Beck *et al.*, Nucl. Instrum. Methods B **126**, 374 (1997).
17. G. Audi, A.H. Wapstra, Nucl. Phys. A **595**, 409 (1995).
18. G. Audi *et al.*, Ncul. Phys. A **729**, 1 (2003).
19. W. Borchers, PhD Thesis, University of Mainz, 1989.
20. P. Möller *et al.*, At. Data Nucl. Data Tables **59**, 185 (1995).
21. T.R. Werner, J. Dudek, At. Data Nucl. Data Tables **54**, 1 (1995).
22. P.F. Mantinca, W.B. Walters, Phys. Rev. C **53**, R2586 (1996).
23. R. Fossion *et al.*, Nucl. Phys. A **697**, 703 (2002).
24. F. Herfurth *et al.*, Eur. Phys. J. A **15**, 17 (2002).
25. H.B. Mathur *et al.*, Phys. Rev. A **96**, 126 (1975).
26. R.B. Moore, Bull. Am. Phys. Soc., 68 (1960).
27. L. Weestgard *et al.*, Z. Phys. A **275**, 127 (1975).
28. K. Sofia *et al.*, Phys. Rev. C **24**, 1615 (1981).
29. R.F. Parry, PhD Thesis, University of California at Berkeley, 1983.
30. G.D. Alkazov *et al.*, Z. Phys. A **344**, 425 (1993).
31. E. Beck *et al.*, Yellow Report CERN 70-30, Vol. **1**, p. 353, 1970, unpublished.
32. F. Münnich *et al.*, Nucl. Phys. A **224**, 437 (1974).
33. A. Wapstra, private communication.
34. T. Batsch *et al.*, Yellow Report CERN 76-33, Vol. **1**, p. 106, 1976, unpublished.
35. J.M. D'Auria *et al.*, Yellow Report CERN 76-33, Vol. **1**, p. 101, 1976, unpublished.
36. P. Hornshoj *et al.*, Nucl. Phys. A **187**, 599 (1972).
37. R.S. Lee *et al.*, Phys. Rev. C **32**, 277 (1985).
38. J.M. D'Auria *et al.*, Nucl. Phys. A **301**, 397 (1978).
39. G.M. Gowdy *et al.*, Phys. Rev. C **13**, 1601 (1976).
40. D.D. Bogdanov *et al.*, Phys. Lett. A **71**, 67 (1977).